ELSEVIER

Polymer 43 (2002) 5011–5016

polymer

www.elsevier.com/locate/polymer

Solid-state electrolyte nanocomposites based on poly(ethylene oxide), poly(oxypropylene) diamine, mineral clay and lithium perchlorate

Hsien-Wei Chen, Chun-Yi Chiu, Hew-Der Wu, I-Wen Shen, Feng-Chih Chang*

Institute of Applied Chemistry, National Chiao-Tung University, Hsin-Chu 30043, Taiwan, ROC

Received 24 August 2001; received in revised form 1 February 2002; accepted 1 May 2002

Abstract

This work has demonstrated that the addition of specific amount of poly(oxypropylene) diamine (d2000) and mineral clay in the PEO-based electrolyte system can form the high conductivity film at room temperature. Specific interactions among silicate layer, d2000, ether oxygen, and lithium cation have been investigated using differential scanning calorimetry (DSC), alternating current impedance (AC impedance) and Fourier-transform infrared (FT-IR). The DSC characterization confirms that the addition of 25 wt% d2000 is able to produce low T_g and fully amorphous $(PEO)_8LiClO_4$/d2000 electrolyte system which produce the good environment for ionic transfer. Additionally, the incorporation of the mineral clay into the $(PEO)_8LiClO_4$/d2000 electrolyte system can sustain the polymeric mechanical property by its huge surface area and enhance the conductivity due to the specific interaction between silicate layers and lithium cation. FT-IR spectra confirm that the incorporation of the clay is able to dissolve the lithium salts more effectively and resulting to the higher fraction of free anions due to the strong interaction between negative charges of the silicate layers and lithium cations of the lithium salt. © 2002 Elsevier Science Ltd. All rights reserved.

Keywords: Polymeric electrolytes; Mineral clay; Poly(oxypropylene) diamine

1. Introduction

Since the original work of Wright and Armand on the poly(ethylene oxide)/alkali metal salt-based solid electrolytes [1–4], considerable efforts have been devoted to the development of solid polymer electrolytes (SPEs) with high ionic conductivity ($\sim 10^{-4}$ S/cm) and dimensional stability. The major motivation for this interest is the application in rechargeable and high energy density power sources. It is generally agreed that both of these qualities can be achieved by the lithium-based electrochemical systems to configure the battery [5–7]. Poly(ethylene oxide) (PEO)-based polymer electrolytes are still among the most extensively studied polymer ionic conductors due to the beneficial structure in supporting fast ion transport [7–14]. However, a high crystalline phase concentration limits the conductivity of PEO-based electrolytes. Adding the plasticizer to PEO-based electrolytes can increase the chain mobility and further reduces the polymeric crystallinity [15–21]. Nevertheless, the lack of dimensional stability and/or mechanical strength is the major drawback of such plasticized polymer electrolytes. These problems may be particularly overcome by the incorporation of mineral clay. Mineral clay is an inorganic filler with intercalation property. Intercalating polymer in layered clay host can produce huge interfacial area to sustain the mechanical property of polymer electrolyte system [22–24] and imparts salt-solvating power to dissolve the lithium salts. According to our previous study [25], the blend of PEO with clay treated by [poly(oxypropylene) diamine] (trade name is d2000) can form the nanocomposite. In this work, we present a novel polymer electrolyte nanocomposite consisting of $(PEO)_8$-$LiClO_4$/d2000/clay and the conductivity can be achieved at 5×10^{-5} S/cm at room temperature with still dimensional stability. The complicated solid-state interaction between PEO, clay mineral, d2000 and lithium cation will be investigated via differential scanning calorimetry (DSC), alternating current impedance (AC impedance), and Fourier-transform infrared (FT-IR).

---

[*] Corresponding author. Tel.: +886-3-5131512; fax: +886-3-5723764.
E-mail address: changfc@cc.nctu.edu.tw (F.C. Chang).

PII: S0032-3861(02)00326-9

2. Experimental section

2.1. Sample preparation

The PEO has the weight average molecular weight of 200 000 (Aldrich). The lithium perchlorate ($LiClO_4$) (Aldrich) was dried in a vacuum oven at 80 °C for 24 h, and then stored in a desiccator prior to use. Acetonitrile was refluxed at a suitable temperature under nitrogen atmosphere prior to use. Poly(oxypropylene) diamine (trade name d2000, $M_n = 2000$) was purchased from Huntsman Co. in United State. The structure of d2000 is illustrated in Scheme 1.

2.2. Preparation of mineral clay

Half mole the d2000 diamine was acidified by hydrochloric acid. One gram sodium montmorillonite (clay) and 50 ml distilled water were placed in a 100 ml beaker, 2.3 g of the acidified d2000 was added to the solution (clay/d2000 = 1/1). The mixture was stirred vigorously for 8 h, and then filtered and washed with deionized water. The modified clay was dried in a vacuum oven at 60 °C for 24 h. Notably, the d2000 modified montmorillonite is highly hydrophobic.

2.3. Preparation of solid polymer electrolyte

Desired amount of PEO, vacuum dried $LiClO_4$ salt, and clay in dry acetonitrile were mixed to form PEO/clay/$LiClO_4$ nanocomposites of varying compositions. Following continuous stirring for 24 h at 70 °C, the mixture was cast on the Teflon plate and maintained at 50 °C for an additional 24 h to facilitate initial de-solvent. Further drying was carried out under vacuum at 70 °C for 3 days. To prevent contact with air and moisture, all nanocomposites were stored in a dry box filled with nitrogen. The quantity of the lithium salt was calculated at $EO/Li^+ = 8$ in this study.

2.4. Differential scanning calorimetry

Thermal analysis was carried out on a DSC instrument from Du-Pont (DSC-9000) with a scan rate of 10 °C/min ranging from −100 to 200 °C. Approximately 5–10 mg of each sample was weighted and sealed in an aluminum pan for DSC analysis. The sample was quickly cooled to −100 °C from the melt state (140 °C) for the first scan and then scanned between −100 and 200 °C at 10 °C/min.

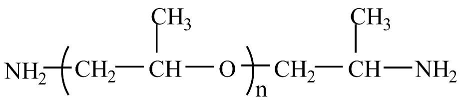

$NH_2-\!\!\left(CH_2-\underset{}{\overset{CH_3}{\overset{|}{CH}}}-O\right)_n\!\!-CH_2-\overset{CH_3}{\overset{|}{CH}}-NH_2$

Scheme 1. The structure of poly(oxypropylene) diamine (d2000).

2.5. Conductivity measurements

Ionic conductivity measurements with alternating current were conducted on a AUTOLAB designed by Eco Chemie within the frequency range from 10 MHz to 10 Hz. The composite film was sandwiched between stainless steel blocking electrodes (1 cm diameter). The specimen thickness varied from 0.8 to 1.2 mm, and the impedance response was gauged over the range from 20 to 120 °C.

2.6. Infrared spectroscopy

The conventional NaCl disk method was employed to measure infrared spectra of composite films. All polymer films were prepared under N_2 atmosphere. The acetonitrile solution was cast onto a NaCl disk from which the solvent was removed under vacuum at 70 °C for 48 h and then stored in the dry box for 2 h. All infrared spectra were obtained at a resolution of 1 cm^{-1} on a Nicolet AVATAR 320 FTIR Spectrometer at 25 °C.

3. Results and discussions

3.1. DSC studies

Fig. 1 presents the DSC thermograms of plain d2000, $(PEO)_8LiClO_4$, and $(PEO)_8LiClO_4$/d2000 (25 wt% d2000) electrolytes. The thermogram of the $(PEO)_8LiClO_4$ shows a exothermic peak at 40.7 °C and endothermic peak at 60.4 °C, corresponding to the recrystallization and melting of the PEO, respectively. The glass transition temperature (T_g) of the PEO can also be found approximately at −14 °C. After the addition of d2000, the T_g of the blend decreases to −23 °C (Fig. 1(b)), implies higher chain mobility of the PEO. No recrystallization exotherm and melt endotherm can be found from this $(PEO)_8LiClO_4$/d2000 composite system.

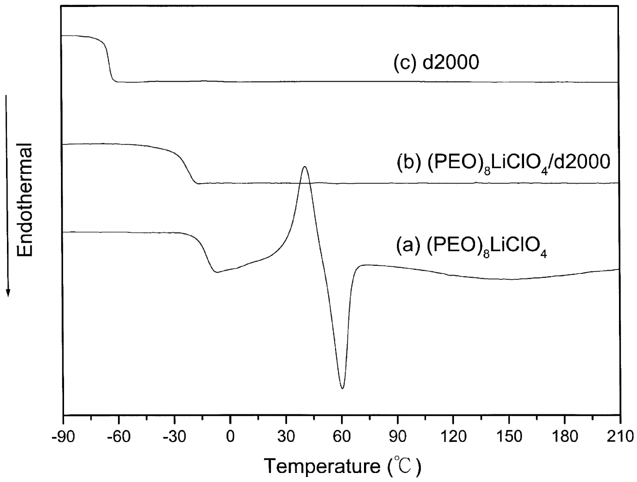

Fig. 1. DSC trances obtained for PEO-based electrolytes system: (a) $(PEO)_8LiClO_4$, (b) $(PEO)_8LiClO_4$/d2000, and (c) d2000.

Therefore, the d2000 plays a role of a plasticizer in the PEO-based electrolyte system to enhance PEO chain mobility and results in lower T_g of the blend. In addition, the cold crystallization behavior of the PEO is inhibited with the addition of d2000 and this phenomenon could be attributed to the hydrogen bonding interaction between the amino group of d2000 and ether group of PEO. This polymeric electrolyte containing 25 wt% d2000 is a softer amorphous system, which is beneficial for ionic transference. Fig. 1(c) shows the thermogram of the d2000. The T_g appears at -65 °C, but no recrystallization exotherm and melt endotherm can be found, implying that the d2000 is a rubbery and fully amorphous polymer.

Fig. 2 presents the T_g trends for the $(PEO)_8LiClO_4$ and $(PEO)_8LiClO_4$/d2000 electrolyte systems with different clay concentrations. As shown in Fig. 2(a), the T_g decreases gradually with increasing clay content. However, the T_g in Fig. 2(b) is essentially unchanged. Fig. 3 plots T_g against clay content (wt%) for $(PEO)_8LiClO_4$ and $(PEO)_8LiClO_4$/d2000 electrolyte systems. This phenomenon can be interpreted as the Lewis base–acid type interactions among polyether matrix, clay filler, lithium cation and corresponding anion. T_g increasing with the incorporation of $LiClO_4$ can be attributed to the formation of transient cross-links between the salt and the polyether phase. According to our prior studies [25,26], clay is a natural mineral with high dielectric constant. The clay mineral can dissolve lithium cations because these silicate layers of the clay play the role of a Lewis base to complex with the lithium cations. With the addition of clay, fraction of the original lithium cation interacting with silicate layers induces higher PEO chain flexibility and thus lower T_g shown in Fig. 3(a). However, a significant difference is observed when 25 wt% d2000 is incorporated. No significant change is observed in T_g varying clay content for the system. This insignificant changed phenomenon in T_g could be thought that the d2000 reduce the interaction between the lithium cation and PEO.

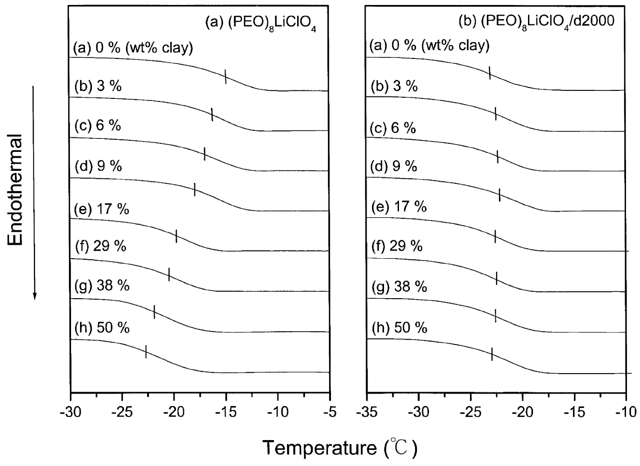

Fig. 2. The trances of T_g varied with clay concentration (wt%) for different PEO-based electrolytes system: (a) $(PEO)_8LiClO_4$ and (b) $(PEO)_8LiClO_4$/-d2000.

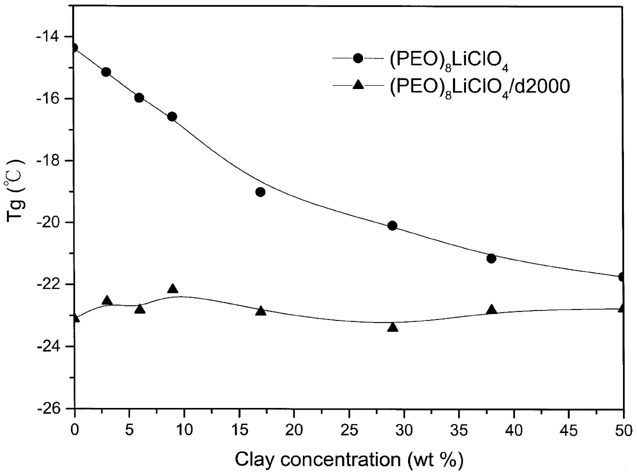

Fig. 3. T_g versus clay concentration (wt%) for different PEO-based electrolytes system: (●) $(PEO)_8LiClO_4$; (▲) $(PEO)_8LiClO_4$/d2000.

Fig. 4 records the FT-IR spectra ranging from 1500 to 700 cm^{-1} of d2000 and d2000/$LiClO_4$ complex. As shown in the d2000 curve, the major peak at 1100 cm^{-1} can be assigned as the COC stretch (ν(COC)). With the addition of the lithium salts, the major peak (~ 1100 cm^{-1}) shifts to lower frequency, indicating that the electron surrounding the ether group of d2000 has been deprived by the lithium cation. Furthermore, the d2000 can complex with the lithium cation via the Lewis acid–base interaction. The inclusion of the d2000 in the $(PEO)_8LiClO_4$ system not only plays the plasticizer role to lubricate the PEO chain but also interacts with the lithium cation to diminish the transient cross-linking effect of the salt with PEO chains. Since the PEO chain in the $(PEO)_8LiClO_4$/d2000 system is flexible and the clay effect in lowering PEO T_g is not significant.

3.2. Conductivity

Fig. 5 presents the Arrhenius plots, which illustrate the

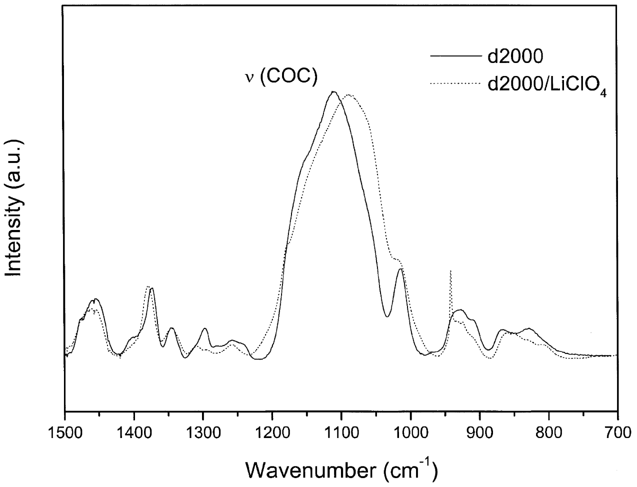

Fig. 4. Infrared spectrum of COC stretching region for d2000 and d2000/$LiClO_4$ complex in the spectral region between 1500 and 700 cm^{-1}.

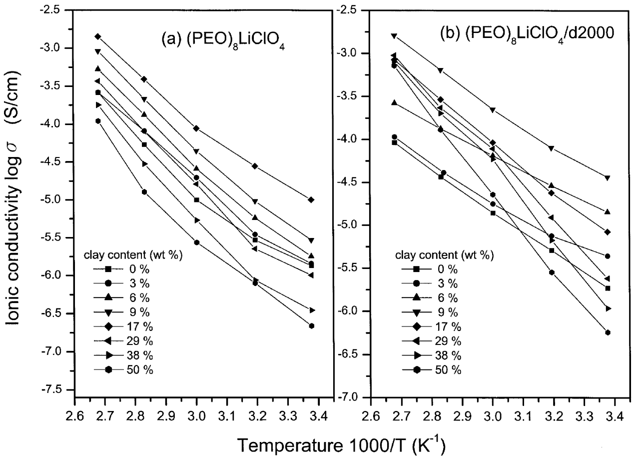

Fig. 5. Arrhenius conductivity plots for different PEO-based electrolytes system with various clay content: (a) $(PEO)_8LiClO_4$ and (b) $(PEO)_8$-$LiClO_4$/d2000.

temperature and clay content dependence on the ionic conductivity for the $(PEO)_8LiClO_4$ and $(PEO)_8LiClO_4$/d2000 electrolyte systems. In the $(PEO)_8LiClO_4$ electrolyte system, the conductivity increases with the increase of the clay content and approaches a maximum when the clay concentration is at 17 wt%. Subsequently, the conductivity decreases drastically with further increase in the clay content. The same trend can also be found in the $(PEO)_8$-$LiClO_4$/d2000 electrolyte system (Fig. 5(b)), but the maximum conductivity appears at 9 wt% clay concentration. Fig. 6 plots of ionic conductivity versus clay content at 30 °C for the $(PEO)_8LiClO_4$ and $(PEO)_8LiClO_4$/d2000 systems. In the $(PEO)_8LiClO_4$ system, a rapid increase in the conductivity is observed by adding small quantity of the clay and the maximum ionic conductivity is at 17 wt% clay content. When the clay content is increased to 23 wt%, the conductivity decreases to near its original value. Further increase in clay content, the conductivity decreases even below the original value. For the $(PEO)_8LiClO_4$/d2000 electrolyte system, similar conductivity behavior is observed except that the maximum conductivity is at 9 wt% of the clay.

The negative charges in the silicate layers can interact with lithium cations and disturb the attractive force between the cationic and anionic ions of the lithium salt. Nevertheless, an excess of clay may increase the system's viscosity and thus restricts cationic ions mobility and results in lower ionic conductivity. From the equation

$$\sigma = \sum_i n_i z_i \mu_i$$

where n_i, z_i, and μ_i refer to the number of the charge carrier, ionic charge and ionic mobility. According to the above equation, the ionic conductivity depends on the amount of charge carriers (n_i) in the system and the mobility (μ_i) of the various species. Addition of the clay can increase the fraction of 'free' anions (increase n_i), meanwhile, the ionic mobility may be reduced (decrease μ_i) owing to the higher viscosity of clay concentration. These two adverse and competitive effects occur in this system, one is favorable and other is unfavorable for ionic conductivity. It can be concluded that the addition of optimum clay content provides the most suitable environment for the ionic transportation and achieves the highest conductivity.

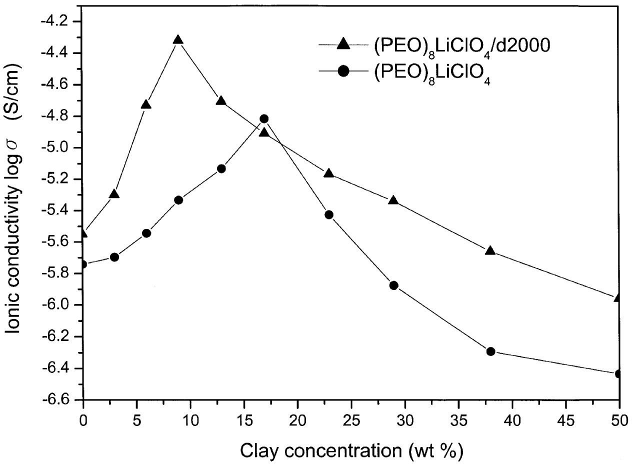

Fig. 6. Ionic conductivity versus clay concentration (wt%) for different PEO-based electrolytes system at 25 °C: (•) $(PEO)_8LiClO_4$; (▲) $(PEO)_8$-$LiClO_4$/d2000.

Additionally, the plain $(PEO)_8LiClO_4$ electrolyte system requires 17 wt% of clay content to attain the maximum conductivity and this critical clay content is higher than that of $(PEO)_8LiClO_4$/d2000 electrolyte system (9 wt%). According to FT-IR results (Fig. 4), the shift of the optimized clay content of the $(PEO)_8LiClO_4$/d2000 electrolyte system can be attributed to the interaction between the d2000 and the lithium cation. In this system, portion of the clay is replaced by the d2000. In order to further clarify the interaction mechanism, Fig. 7 illustrates the various

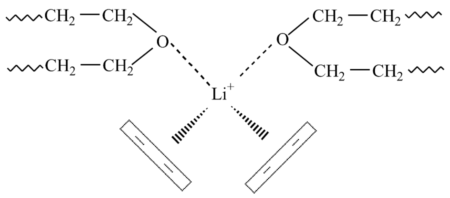

(a) complex type I

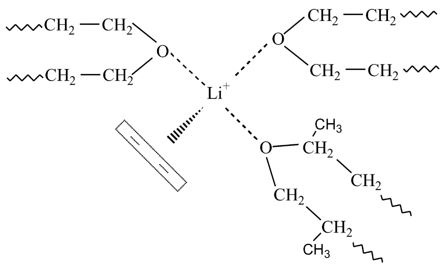

(b) complex type II

Fig. 7. Schematic structure of the complexes formed by Li^+ cation with (a) polyether and silicate layers (type I complex) and (b) polyether, silicate layers and d2000 (type II complex).

complex schemes. In the $(PEO)_8LiClO_4$ electrolyte system, the clay and the ether group of the PEO interact with the lithium cation simultaneously to form the type I complex. When the d2000 is added to the $(PEO)_8LiClO_4$ electrolyte system, portion of the original lithium cation interacts with d2000 to form the type II complex. Therefore, the $(PEO)_8LiClO_4$/d2000 system requires less clay content to form the optimized equilibrium attraction force than the $(PEO)_8LiClO_4$ electrolyte system.

In the $(PEO)_8LiClO_4$/d2000 electrolyte system at 30 °C and 9 wt% clay, the conductivity is 4.8×10^{-5} S/cm which is approximately 17 times higher than the blank electrolyte system. On the other hand, in the $(PEO)_8LiClO_4$ electrolyte system at 30 °C and 17 wt% clay, the maximum conductivity is 1.5×10^{-5} S/cm which is only eight times higher than the blank electrolyte system. Fig. 6 clearly demonstrates that the conductivity of the $(PEO)_8LiClO_4$/d2000 electrolyte system is higher than the $(PEO)_8LiClO_4$ electrolyte system.

3.3. FT-IR spectroscopy

FT-IR spectroscopy is a powerful tool for probing microscopic details in electrolytic systems. The characteristic $\nu(ClO_4^-)$ mode of the lithium perchlorate ($LiClO_4$) is particularly sensitive in changing the local anionic environment [14,27–29]. According to prior literature [14,29], the component observed at $\sim 624\ cm^{-1}$ has been assigned to the free anion which does not interact directly with lithium cation. Component at $\sim 635\ cm^{-1}$ has been attributed to contact ion pair. Fig. 8 shows the typical infrared spectra in the $\nu(ClO_4^-)$ spectral ranging from 650 to 600 cm^{-1} containing various clay concentrations for $(PEO)_8LiClO_4$ and $(PEO)_8LiClO_4$/d2000 binary blends at 30 °C where a large adsorption band at $\sim 624\ cm^{-1}$ and a shoulder at $\sim 635\ cm^{-1}$ appear. As shown in Fig. 8(a), the shoulder at $\sim 635\ cm^{-1}$ decreases gradually with increasing clay concentration and nearly disappears when the clay is 17 wt%. However, the identical trend can also be observed in the $(PEO)_8LiClO_4$/d2000 systems [Fig. 8(b)]. The free anion band ($\sim 635\ cm^{-1}$) approximately disappears when small amount of clay was added and maintain the constant value with further increase in clay concentration.

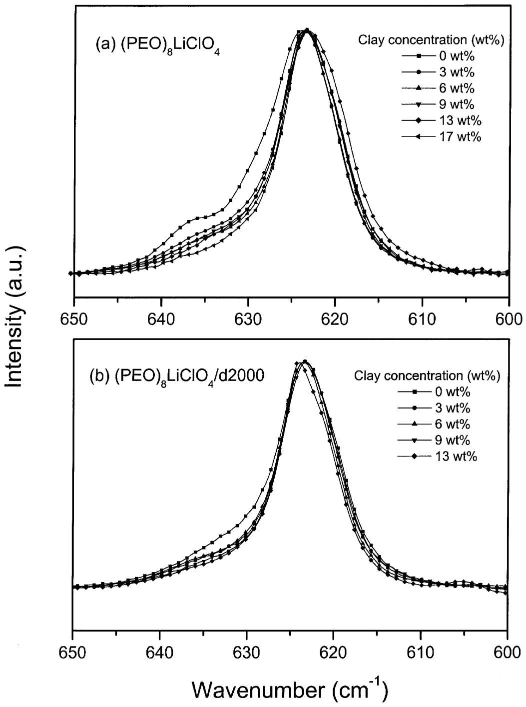

Fig. 8. Infrared spectra of $\nu(ClO_4^-)$ internal modes versus clay concentration (wt%) for different PEO-based electrolytes system at 25 °C: (a) $(PEO)_8LiClO_4$ and (b) $(PEO)_8LiClO_4$/d2000.

In order to further clarify the clay effect in dissolving the lithium salts, relative fraction of the free anions are measured by decompositing the $\nu(ClO_4^-)$ band into two Gaussian peaks with peak centered at 624 and 635 cm^{-1}, respectively. An example is shown in Fig. 9 for the $(PEO)_8LiClO_4$ based electrolyte systems where fractions of free anions and contact ion pairs were calculated as the ratio of the area under respective peaks to the total area for the $\nu(ClO_4^-)$ vibration. Fig. 10 presents the relative fractions of free anions with various clay concentrations determined by curve fitting. It is clear seen that the relative fractions of the free anions increase with clay concentration. In other words, the addition of the clay can facilitate the system to dissolve the lithium salts. The phenomenon is consistent to the T_g and conductivity results and it can be attributed to the specific interaction between silicate layers of the clay and the lithium cations. As shown in the $(PEO)_8LiClO_4$ system, the fraction of free anions has a strong clay concentration dependence at lower clay content (< 17 wt%), a nearly linear relationship is evident. However, in the $(PEO)_8LiClO_4$/d2000 system, the fraction of free anions increases more rapidly when small amount of clay is incorporated (< 3 wt%) and approaches a plateau at about 13 wt%. It can

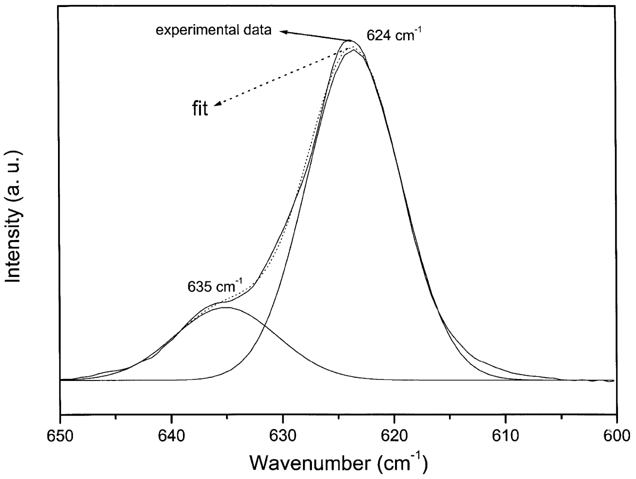

Fig. 9. Peak fitting of the $\nu(ClO_4^-)$ FT-IR internal modes for the $(PEO)_8LiClO_4$ system at 25 °C.

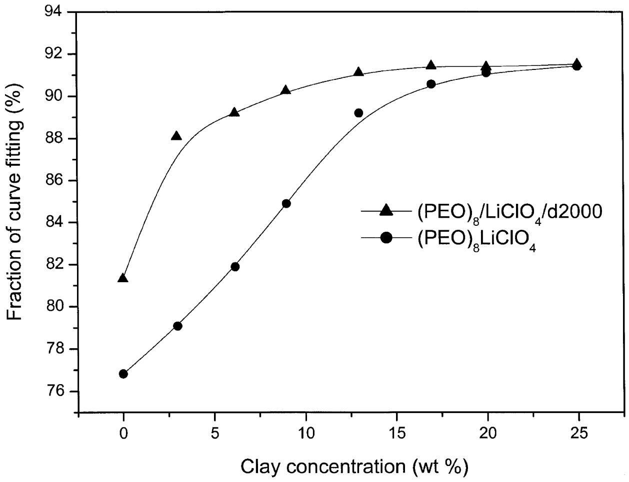

Fig. 10. Fraction of free anion versus clay concentration (wt%) for different PEO-based electrolytes system at 25 °C: (•) $(PEO)_8LiClO_4$ and (▲) $(PEO)_8LiClO_4$/d2000.

be considered as that the clay effect in dissolving the lithium salts is more significant (require less clay concentration) when 25 wt% d2000 is added. According to Figs. 4 and 7, the d2000 can complex with the lithium salts and the Complex I tends to shift into Complex II with the addition of the d2000 to the $(PEO)_8LiClO_4$ electrolyte system. Furthermore, the Complex II requires less clay mineral to dissolve the lithium salts that can be expected. The fraction of free anions at high concentration of clay does not vary significantly in both systems because essentially all lithium salts have been dissolved.

4. Conclusions

This study has demonstrated that the addition of optimum content of montmorillonite to the $(PEO)_8LiClO_4$/-d2000 electrolyte system is able to form high conductivity films of 5×10^{-5} S/cm at room temperature. DSC results indicate that the addition of 25 wt% d2000 can retard the PEO crystallinity producing the softer and amorphous environment. Furthermore, DSC, AC impedance and FT-IR studies indicated that the complicated interactions occur between the silicate layer, d2000 and the $LiClO_4$ within the PEO/d2000/$LiClO_4$/clay composite electrolyte system. The presence of d2000 tends to form type II complex at the cost of type I complex by drawing lithium cation away from the PEO–clay region. The negative charges on the silicate layers and d2000 can dissolve the lithium salts simultaneously due to the same function as the polar group in PEO. FT-IR spectra had demonstrated that the addition of clay can dissolve the lithium salt effectively and results in higher fraction of free anions and higher ionic conductivity. The addition of d2000 and clay in the PEO-based electrolyte system can overcome the kinetic (lower T_g) and thermodynamic (dissolve the lithium ions) hindrance and produces a good environment for the lithium transference. Balanced attractive forces among silicate layers, d2000, ether groups and lithium cations is able to produce an optimum ionic conductivity.

References

[1] Fenton DE, Parker JM, Wright PV. Polymer 1973;3:589.
[2] Wright PV. Br Polym J 1975;7:319.
[3] Armand MB. Solid State Ionics 1983;9–10:745.
[4] Armand MB. Annu Rev Mater Sci 1986;16:245.
[5] Jiang Z, Alamgir M, Abraham KM. J Electrochem Soc 1995;142:3333.
[6] Scrosati B. In: MacCallum JR, Vincent CA, editors. Polymer electrolyte reviews. New York: Elsevier; 1989. p. 315.
[7] Wieczorek W, Zalewska A, Raducha D, Florjanczyk Z, Stevens JR. Macromolecules 1996;29:143.
[8] Wieczorek W, Raducha D, Zalewska A, Stevens JR. J Phys Chem B 1998;102:8725.
[9] Scrosati B. In: Scrosati B, editor. Applications of electroactive polymers. New York: Chapman & Hall; 1993. p. 251.
[10] Abraham KM, Jiang Z, Carroll B. Chem Mater 1997;9:1978.
[11] Yang XQ, Hanson L, McBreen J, Okamoto Y. J Power Source 1995;54:198.
[12] Lee JC, Litt MH. Macromolecules 2000;33:1618.
[13] Labreche C, Levesque I, Prud'homme J. Macromolecules 1996;29:7795.
[14] Mishra R, Rao KJ. Solid State Ionics 1998;106:113.
[15] Bandara LRAK, Dissanayake MAKL, Mellander BE. Electrochim Acta 1998;43:1447.
[16] Jaipal Reddy M, Sreekanth T, Subba Rao UV. Solid State Ionics 1999;126:55.
[17] Sukeshini AM, Kulkarni AR, Sharma A. Solid State Ionics 1998;113–115:179.
[18] Chintapalli S, Frech R. Solid State Ionics 1996;86:341.
[19] Frech R, Chintapalli S. Solid State Ionics 1996;85:61.
[20] Chintapalli S, Frech R. Macromolecules 1996;29:3499.
[21] Kovač M, Gaberšček M, Grdadolnik. Electrochim Acta 1998;44:863.
[22] Harries DJ, Bonagamba TJ, Schmidt-Rohr K. Macromolecules 1999;32:6718.
[23] Jeevanandam P, Vasudevan S. Chem Mater 1998;10:1276.
[24] Ruiz-Hitzky E, Galvan JC, Merino J, Casal B, Aranda P, Jimenez-Morales A. Solid State Ionics 1996;85:313.
[25] Chen HW, Chang FC. Polymer 2001;42:9763.
[26] Chen HW, Chang FC. J Polym Sci, Part B: Polym Phys 2001;39:2407.
[27] Xuan X, Wang J, Tang J, Qu G, Lu J. Spectrochim Acta Part A 2000;56:2131.
[28] Wang Z, Huang B, Huang H, Chen L, Xue R. Solid State Ionics 1996;85:143.
[29] Salomon M, Xu M, Eyring EM, Petrucci S. J Phys Chem 1994;98:8234.